ISSN: 2688-8645

High-Temperature Performance of Ultra-High-Performance Concrete Incorporating Iron Tailings Sand and Steel Slag Powder

Shibo Tian, Bo Liu

North China University of Science and Technology, Tangshan, Hebei, 063210, China

Abstract

Ultra-high-performance concrete (UHPC) incorporating iron tailings sand and steel slag powder was prepared to investigate the effects of steel–polypropylene (PP) fiber proportions on flowability, ambient mechanical properties, and post-heating residual strength. The total fiber volume fraction was maintained at 2.0%, with PP fiber volume fractions of 0, 0.3%, 0.6%, and 0.9%. The steel-fiber mixture and the mixture containing 1.7% steel fibers and 0.3% PP fibers were selected for exposure to 200, 400, 600, and 800 °C at a heating rate of 4 °C/min, followed by a 2 h holding period and natural cooling. Increasing the PP fiber fraction reduced the flow spread from 489 to 442 mm. The mixture containing 0.3% PP fibers largely retained its ambient strength, with 28-day compressive and flexural strengths of 117.3 and 19.7 MPa, respectively. Both selected mixtures exhibited their highest residual strengths at the tested temperature of 200 °C, followed by strength reductions at higher temperatures. The steel-fiber specimens lost structural integrity after exposure to 600 °C, whereas the PP-containing specimens remained intact without thermal spalling at 600 and 800 °C. Nevertheless, their residual compressive and flexural strengths decreased to 19.8 and 3.9 MPa, respectively, at 800 °C. These results show that specimen integrity and residual load-bearing capacity must be evaluated separately when selecting fiber combinations for heat-exposed UHPC.

Keywords

Ultra-high-performance Concrete; Iron Tailings Sand; Steel Slag Powder; Hybrid Fibers.

1. Introduction

Ultra-high-performance concrete (UHPC) achieves a dense matrix and enhanced mechanical performance through optimized particle packing, a low water-to-binder ratio, and fiber reinforcement. The combined design of mineral additions and fibers has become an important means of tailoring its workability, mechanical properties, and durability [1]. However, the substantial demand for cement and high-quality fine aggregate in conventional UHPC increases material costs and resource consumption. Replacing part of these constituents with industrial solid wastes is therefore of practical interest [2].

Iron ore tailings can be used as fine aggregate in UHPC, although complete replacement of natural fine aggregate can substantially reduce workability and compressive strength [3]. In a study replacing manufactured sand with iron ore tailings, a mass replacement ratio of 40% produced the highest compressive strength, while resistance to water penetration improved as the tailings content increased [4]. For the binder system, the combined use of steel slag powder and an expansive agent was reported to modify hydration heat release and shrinkage, although some strength loss occurred [5]. An appropriate steel slag powder replacement level can improve mechanical performance by modifying particle packing and the fiber–matrix interface; excessive replacement can impair hydration and interfacial bonding [6].

The dense, low-permeability microstructure of UHPC can restrict water-vapor transport during heating and increase the risk of explosive spalling. Polymer fibers provide a means of modifying

ISSN: 2688-8645

transport properties at elevated temperatures. Thermal mismatch between polypropylene (PP) fibers and the surrounding matrix can generate interconnected microcracks before fiber melting; consequently, spalling mitigation is not solely attributable to the voids left by melted fibers [7]. Under specific experimental conditions, hybrid steel and PP fibers can improve connectivity between microcracks and fiber channels and effectively mitigate spalling. Their effectiveness also depends on the length, aspect ratio, and volume fraction of the PP fibers [8, 9].

Although steel–polyethylene hybrid fibers can improve ambient flexural behavior, their effectiveness in mitigating spalling is limited. Improvements in ambient toughness therefore cannot be directly equated with improved performance after heat exposure [10]. Different synthetic fibers also make different contributions to spalling resistance and residual mechanical properties [11]. Recent studies of steel–polyoxymethylene and steel–polyethylene–PP hybrid systems further indicate that fiber type and proportion must be coordinated to balance spalling mitigation, crack control, and residual load-bearing capacity [12, 13].

When iron tailings sand and steel slag powder are incorporated together, changes in particle packing, hydration products, and pore structure may affect thermal damage in hybrid-fiber UHPC. Systematic consideration of replacement levels, fiber proportions, and heating conditions is therefore needed to clarify their combined effects on spalling and residual strength. The present study examines the effects of steel–PP fiber proportions at a fixed mineral composition, with particular attention to flowability, ambient strength development, and residual mechanical properties after heat exposure.

2. Materials and Methods

2.1. Raw Materials

The UHPC mixtures were prepared using PII 52.5R Portland cement (Conch), steel slag powder, silica fume, quartz sand, silica-rich iron tailings sand from Qian'an, Tangshan, Hebei Province, China, water, and a polycarboxylate-based high-range water-reducing admixture. The aggregate properties are listed in Table 1, the mixture proportions in Table 2, the fiber properties in Table 3, and the admixture properties in Table 4.

Table 1. Physical properties of the aggregates

Aggregate type	Apparent density (g/cm^3)	Bulk density (g/cm^3)	Void content (%)	Fineness modulus
ITS	2.51	1.61	35.90%	2.73
QS	2.52	1.68	33.20%	2.89

Before mixing, the aggregates were oven-dried at 105 °C for 2 h and then allowed to cool.

Table 2. Mixture proportions of the UHPC mixtures

Mixture	Mass ratio relative to cement						w/b	SF (vol.%)	PP (vol.%)	PVA (vol.%)	PA (vol.%)
	C	SSP	SiF	QS	ITS	SP					
SF2.0	1	0.42	0.25	1	0.67	0.02	0.18	2.0			
SF1.7-PP0.3	1	0.42	0.25	1	0.67	0.02	0.18	1.7	0.3		
SF1.4-PP0.6	1	0.42	0.25	1	0.67	0.02	0.18	1.4	0.6		
SF1.1-PP0.9	1	0.42	0.25	1	0.67	0.02	0.18	1.1	0.9		

ISSN: 2688-8645

C: cement; SSP: steel slag powder; SiF: silica fume; QS: quartz sand; ITS: iron tailings sand; SP: superplasticizer; W: water; w/b: water-to-binder ratio; SF: steel fibers; PP: polypropylene fibers; PVA: polyvinyl alcohol fibers; PA: polyamide fibers.

Table 3. Physical and mechanical properties of the fibers

Fiber type	Length (mm)	Diameter (mm)	Aspect ratio	Density (kg/m^3)	Tensile strength (MPa)	Melting point (°C)
SF	16	0.22	72	7850	2000	1450
PP	9	0.03	300	910	500	170

Table 4. Physicochemical properties of the water-reducing admixture

Property	Value
Admixture type	Polycarboxylate ether (PCE)-based HRWR
Appearance	Milky white powder
pH	6–8
Moisture content	<3%
Total alkali content	<5%
Chloride ion content	<0.03%
Surface tension	71.5–72.0
Recommended dosage	0.16–0.3% by mass of binder
Compatibility	Suitable for UHPC, fiber-reinforced systems, and high-fluidity concrete

2.2. Test Methods

2.2.1. Flowability

The flowability of fresh UHPC was measured in accordance with GB/T 50080-2016 [14]. The slump cone was filled with the mixture and then lifted steadily over 3–7 s. Once spreading ceased, or after 90 s, the maximum spread diameter and the diameter perpendicular to it were measured. Their mean was taken as the flow spread.

2.2.2. Mechanical Properties

Compressive and flexural strengths before and after heat exposure were determined using a YAS-5000 electrohydraulic servo testing machine in accordance with GB/T 31387-2015 [15]. The stress application rates were 1.0 MPa/s for compression and 0.1 MPa/s for flexure. Three specimens were used for each strength determination. A flexural loading fixture was used with a shear-span-to-depth ratio of β = 3. The residual strength retention was calculated using Eq. (1).

$$R_s = \frac{F_{ht}}{F_{rt}} \times 100\% \quad (1)$$

where R_s is the residual strength retention (%), F_{ht} is the strength after heat exposure (MPa), and F_{rt} is the strength at room temperature (MPa).

2.2.3. Heat-exposure Tests

Specimens cured for 28 days were pre-dried in a forced-air oven at 105 °C for 24 h and weighed. Drying was continued in successive 24 h cycles until the mass loss between two consecutive cycles was less than 0.2%.

The target temperatures were 200, 400, 600, and 800 °C. The specimens were heated at 4 °C/min, held at the target temperature for 2 h, and then allowed to cool naturally to room temperature.

ISSN: 2688-8645

3. Results and Discussion

3.1. Flowability

The flowability results are shown in Fig. 1. Increasing the PP fiber fraction while decreasing the steel fiber fraction progressively reduced the flow spread. The SF2.0 mixture exhibited the largest flow spread, 489 mm. The SF1.7-PP0.3, SF1.4-PP0.6, and SF1.1-PP0.9 mixtures reached 468, 453, and 442 mm, respectively, corresponding to reductions of 4.29%, 7.36%, and 9.61% relative to SF2.0. Thus, within the mixture compositions and fiber proportions investigated, replacing part of the steel fibers with PP fibers reduced flowability.

At a given fiber volume, the finer PP fibers used in this study provide a greater number of individual fibers and a larger total surface area. More paste is required to coat the fibers, increasing resistance to flow.

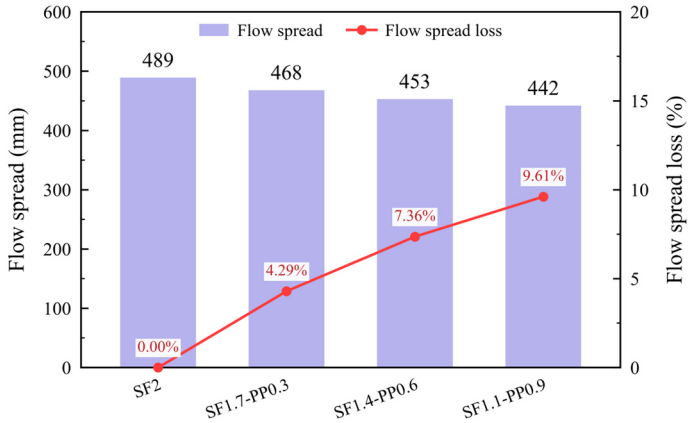


Fig 1. Flow spread and its reduction relative to SF2.0 for the four UHPC mixtures

3.2. Compressive Strength at Ambient Temperature

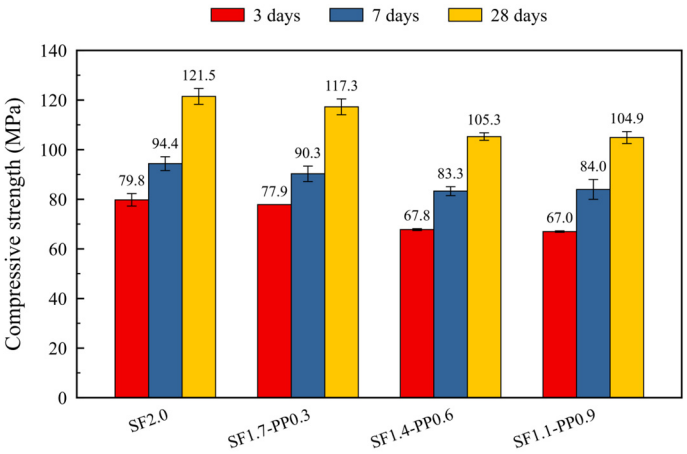


Fig 2. Compressive strength of the UHPC mixtures at different ages

The compressive strengths at different ages are presented in Fig. 2. All four mixtures exhibited increasing compressive strength with age, and SF2.0 had the highest strength at each age. Relative to SF2.0, the compressive strengths of SF1.7-PP0.3 decreased by 2.38%, 4.34%, and 3.46% at 3, 7, and 28 days, respectively. These relatively small reductions indicate that this fiber combination largely retained the ambient compressive strength of the reference mixture.

The 28-day compressive strengths of SF1.4-PP0.6 and SF1.1-PP0.9 decreased to 105.3 and 104.9 MPa, respectively, corresponding to reductions of 13.33% and 13.66% relative to SF2.0.

ISSN: 2688-8645

Steel fibers have a high elastic modulus and can bridge cracks developing under compression. Reducing the steel fiber fraction while increasing the fraction of low-modulus PP fibers may weaken this restraint, contributing to the observed reduction in compressive strength.

3.3. Flexural Strength at Ambient Temperature

The flexural strengths of the four mixtures are shown in Fig. 3. Flexural strength increased with age for every mixture. Between 3 and 28 days, the strengths of SF2.0, SF1.7-PP0.3, SF1.4-PP0.6, and SF1.1-PP0.9 increased from 13.5, 12.15, 11.85, and 10.4 MPa to 20.9, 19.7, 16.8, and 16.4 MPa, respectively.

At 28 days, flexural strength decreased progressively as the PP fiber fraction increased and the steel fiber fraction decreased. The three hybrid-fiber mixtures exhibited reductions of 5.7%, 19.6%, and 21.5%, respectively, relative to SF2.0. SF1.7-PP0.3 retained a flexural strength close to that of the steel-fiber mixture, whereas larger reductions occurred in SF1.4-PP0.6 and SF1.1-PP0.9. Flexural load-bearing capacity depends on crack development in the tensile zone, stress transfer across cracks by fibers, and fiber–matrix interfacial bonding. The high stiffness and strength of steel fibers allow continued load transfer after cracking. Partial replacement with low-modulus PP fibers may reduce the load carried by fibers bridging the cracks.

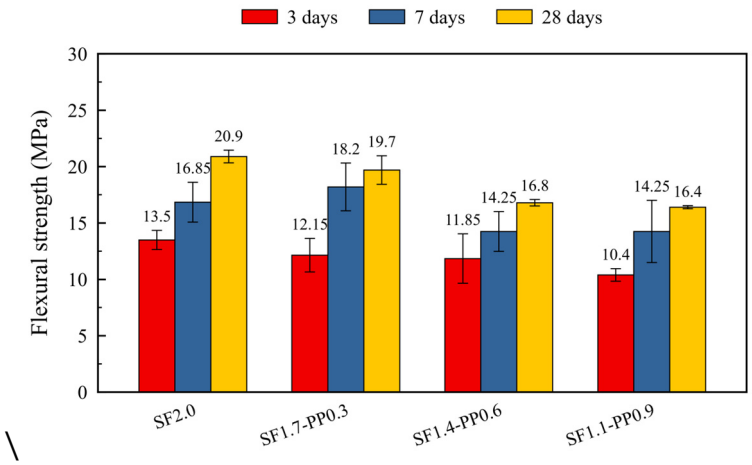


Fig 3. Flexural strength of the UHPC mixtures at different ages

3.4. Residual Compressive Strength after Heat Exposure

The SF2.0 mixture and the SF1.7-PP0.3 mixture, which exhibited favorable ambient mechanical performance, were selected for the heat-exposure tests. They are designated SF and PP, respectively, in Figs. 4 and 5. Both mixtures exhibited an initial increase followed by a decrease in residual compressive strength over the tested range of 20–400 °C, while PP underwent substantial further deterioration at 600–800 °C.

Between 20 and 200 °C, the residual compressive strength of SF increased from 121.7 to 144.5 MPa, an increase of 18.7%, while that of PP increased from 117.5 to 141.3 MPa, an increase of 20.3%. This enhancement may be associated with continued hydration of previously unreacted cementitious constituents under the heating conditions, improving the matrix structure.

Between 200 and 400 °C, the strengths decreased. SF reached 129.2 MPa, 10.6% below its value at 200 °C, while PP reached 129.3 MPa, a reduction of 8.5%. The two mixtures had similar strengths at 400 °C, and both remained above their respective room-temperature values. Dehydration of hydration products and the development of microcracks may progressively offset the earlier strength enhancement.

At higher temperatures, PP exhibited substantial compressive strength loss. Its residual strength decreased from 129.3 MPa after exposure to 400 °C to 73.4 MPa at 600 °C and 19.8

ISSN: 2688-8645

MPa at 800 °C. The corresponding retention values relative to its room-temperature strength were 62.5% and 16.9%. Thus, the enhancement observed at lower temperatures did not persist, and matrix deterioration increasingly governed the residual load-bearing capacity. Possible contributing processes include further dehydration and decomposition of hydration products, weakening of interfacial bonding, and crack propagation. After exposure to 600 °C, SF exhibited surface spalling and exposed steel fibers and lost structural integrity.

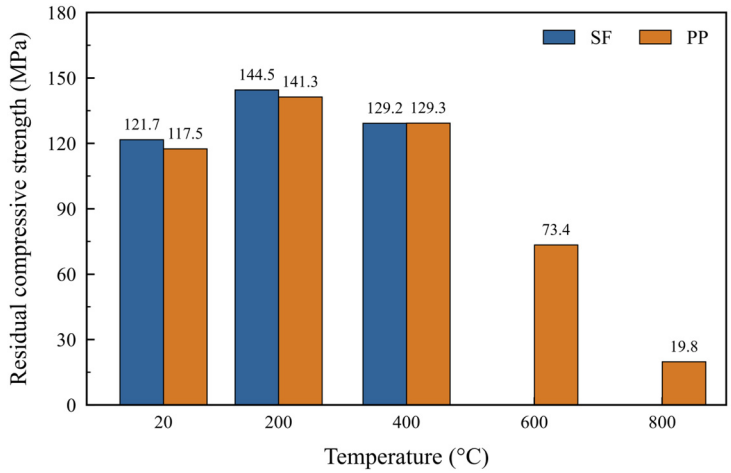


Fig 4. Residual compressive strength of SF and PP after heat exposure

3.5. Residual Flexural Strength after Heat Exposure

Among the tested temperatures, both mixtures exhibited their highest residual flexural strengths after exposure to 200 °C, with increases of 15.3% for SF and 16.2% for PP relative to their respective room-temperature values (Fig. 5). After exposure to 400 °C, the strengths decreased by 14.5% and 18.6%, respectively, relative to their values at 200 °C, indicating that the earlier strength enhancement had been offset by progressive thermal damage.

PP exhibited substantial deterioration between 400 and 800 °C. Its residual flexural strength decreased from 21.0 MPa at 400 °C to 10.0 MPa at 600 °C and 3.9 MPa at 800 °C, corresponding to cumulative losses of approximately 55.0% and 82.4% relative to room temperature. The strength enhancement at lower temperatures therefore did not persist, and the residual flexural load-bearing capacity was markedly reduced at 600 °C and above. SF specimens lost integrity after exposure to 600 °C and could not be tested in flexure.

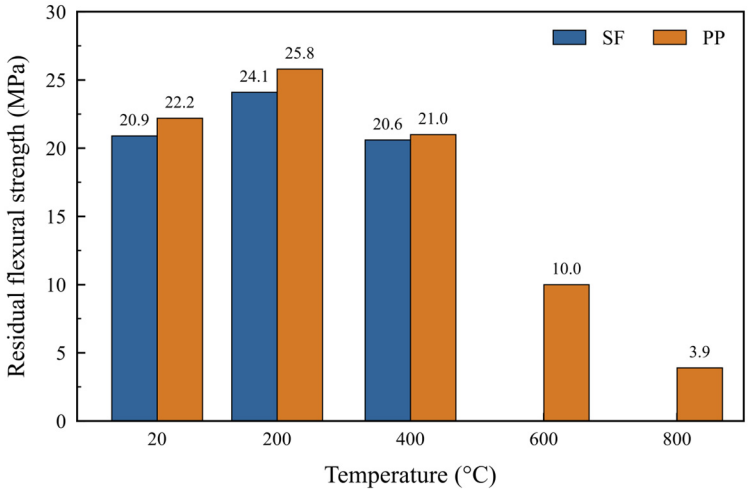
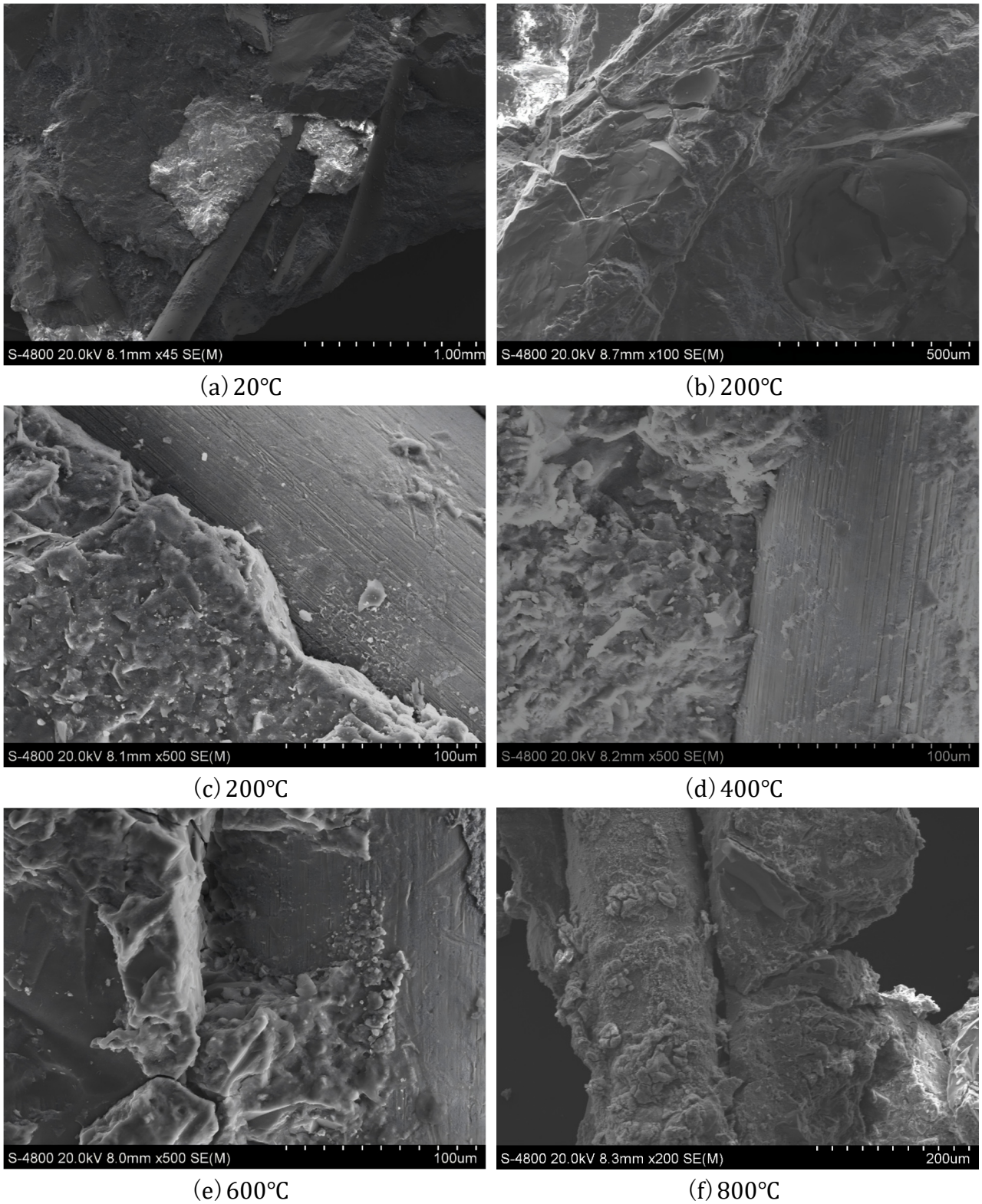


Fig 5. Residual flexural strength of SF and PP after heat exposure

ISSN: 2688-8645

3.6. Microstructural Evolution



(a) 20℃ (b) 200℃

(c) 200℃ (d) 400℃

(e) 600℃ (f) 800℃

Fig 6. Microstructural Evolution

The microstructural evolution of UHPC is shown in Fig 6. At 20 °C, the matrix exhibits a continuous, block-like morphology, with steel fibers embedded within it and cement paste adhering to portions of their surfaces Fig 6(a). At ambient temperature, the steel fibers transfer tensile stresses and bridge cracks. At 200 °C, localized pores or cavities are visible in Fig 6(b), and the melting of PP fibers creates interconnected pore channels that facilitate water vapor

ISSN: 2688-8645

release. In Fig 6(c), the steel fiber surface remains relatively smooth, with clearly visible longitudinal striations and substantial amounts of matrix material still attached. At this stage, free water escapes, and some hydration products begin to dehydrate. The temperature has generally exceeded the melting range of PP fibers, substantially reducing their reinforcing effect, whereas the steel fibers and surrounding matrix retain some stress-transfer capacity. At 400 °C, the steel fiber profile and longitudinal surface striations remain clearly visible Fig 6(d). The adjacent matrix exhibits pronounced accumulations of granular and plate-like material, with localized gaps at the interface. Increasing dehydration and incompatible thermal deformation begin to impair the integrity of both the matrix and the interface. At 600 °C, distinct cracks, lamellar separation, and localized delamination appear in the matrix adjacent to the fibers, indicating poor structural integrity around the interface Fig 6(e). Continued dehydration and decomposition of hydration products, combined with cement paste shrinkage and differences in thermal deformation among the paste, fibers, and aggregates, intensify crack propagation and interfacial debonding. Even when the steel fibers remain intact, the surrounding matrix may no longer provide sufficient anchorage, thereby limiting stress transfer through fiber bridging. At 800 °C, the surfaces of the fiber-like structures are covered with numerous granular deposits, while the adjacent matrix exhibits fragmentation and separation, together with relatively large open voids, indicating severe matrix damage Fig 6(f).

As the temperature increases from 20 to 800 °C, microstructural damage in UHPC progressively develops from localized pore and interfacial changes into matrix cracking, delamination, and fiber–matrix separation. At 200 °C, the steel fiber surfaces remain relatively smooth, with substantial amounts of adjacent matrix material still attached, indicating that the local interface retains a degree of integrity. Meanwhile, the melting of PP fibers and associated interfacial changes may create pathways for water vapor transport. As the temperature rises to 400 °C, matrix dehydration and incompatible thermal deformation among the constituents become more pronounced, and interfacial damage gradually emerges. At 600 °C, distinct cracks and delamination develop in the matrix adjacent to the fibers, indicating further deterioration of steel fiber anchorage. At 800 °C, matrix fragmentation and interfacial separation become more pronounced, and numerous granular deposits, comprising residual cement paste and oxidation products, appear on the steel fiber surfaces.

4. Conclusion

This study investigated how the proportions of steel and polypropylene fibers affect the flowability, ambient mechanical properties, and post-heating residual mechanical properties of UHPC incorporating iron tailings sand and steel slag powder. The following conclusions apply to the materials and experimental conditions investigated.

(1) At a total fiber volume fraction of 2.0%, partial replacement of steel fibers with PP fibers reduced the flowability of fresh UHPC. Increasing the PP fiber volume fraction from 0 to 0.9% decreased the flow spread from 489 to 442 mm, a reduction of 9.61%.

(2) The compressive and flexural strengths of all four mixtures increased with age. A relatively low PP fiber fraction largely retained both the ambient compressive and flexural strengths of this UHPC system.

(3) Over the tested range of 20–400 °C, the residual strengths of SF and PP initially increased and then decreased. The highest compressive and flexural strengths among the tested temperatures were obtained at 200 °C. Relative to their respective room-temperature values, the compressive strengths of SF and PP increased by 18.7% and 20.3%, while their flexural strengths increased by 15.3% and 16.2%. Both strength measures decreased after exposure to 400 °C. SF exhibited surface spalling and exposed steel fibers after exposure to 600 °C, lost structural integrity, and could not undergo subsequent testing. PP remained intact without

thermal spalling after exposure to 600 and 800 °C, but its residual strengths decreased substantially. At 600 and 800 °C, its compressive strengths were 73.4 and 19.8 MPa, with retention values of 62.5% and 16.9%, respectively. Its flexural strengths were 10.0 and 3.9 MPa, with retention values of approximately 45.0% and 17.6%, respectively. The enhancement at lower temperatures did not persist to the higher-temperature regime, where matrix deterioration substantially reduced the residual load-bearing capacity.

(4) As the temperature increases from 20 to 800 °C, damage in UHPC progressively evolves from localized pore and interfacial damage to matrix cracking, delamination, and fiber–matrix debonding. At 200 °C, PP fibers melt, forming channels for water vapor release, while steel fibers retain some interfacial stress-transfer capacity. At 600–800 °C, the dehydration and decomposition of hydration products, together with incompatible thermal deformation among the constituents, intensify matrix and interfacial damage, weakening the anchorage and crack-bridging action of steel fibers. These changes provide a microstructural explanation for the deterioration of UHPC mechanical properties after exposure to elevated temperatures.

Acknowledgments

Supported by the Graduate Student Innovation Fund of North China University of Science and Technology (2026S07).

References

[1] Richard, P., & Cheyrezy, M. (1995). Composition of reactive powder concretes. Cement and Concrete Research, 25(7), 1501–1511. https://doi.org/10.1016/0008-8846(95)00144-2.

[2] Sharma, R., Jang, J. G., & Bansal, P. P. (2022). A comprehensive review on effects of mineral admixtures and fibers on engineering properties of ultra-high-performance concrete. Journal of Building Engineering, 45, 103314. https://doi.org/10.1016/j.jobe.2021.103314.

[3] Zhao, S., Fan, J., & Sun, W. (2014). Utilization of iron ore tailings as fine aggregate in ultra-high performance concrete. Construction and Building Materials, 50, 540–548. https://doi.org/10.1016/j.conbuildmat.2013.10.019.

[4] Zhang, W., Gu, X., Qiu, J., Liu, J., Zhao, Y., & Li, X. (2020). Effects of iron ore tailings on the compressive strength and permeability of ultra high performance concrete. Construction and Building Materials, 260, 119917. https://doi.org/10.1016/j.conbuildmat.2020.119917.

[5] Li, S., Cheng, S., Mo, L., & Deng, M. (2020). Effects of Steel Slag Powder and Expansive Agent on the Properties of Ultra-High Performance Concrete (UHPC): Based on a Case Study. Materials, 13(3), 683. https://doi.org/10.3390/ma13030683.

[6] Piao, R., Kim, S. J., Na, Y. K., Lee, N., & Yoon, Y. S. (2025). Optimization of cement replacement with steel slag powder in ultra-high-performance concrete: Microstructural evolution and mechanical performance. Construction and Building Materials, 492, 142862. https://doi.org/10.1016/j.conbuildmat.2025.142862.

[7] Zhang, D., Dasari, A., & Tan, K. H. (2018). On the mechanism of prevention of explosive spalling in ultra-high performance concrete with polymer fibers. Cement and Concrete Research, 113, 169–177. https://doi.org/10.1016/j.cemconres.2018.08.012.

[8] Li, Y., Tan, K. H., & Yang, E. H. (2019). Synergistic effects of hybrid polypropylene and steel fibers on explosive spalling prevention of ultra-high performance concrete at elevated temperature. Cement and Concrete Composites, 96, 174–181. https://doi.org/10.1016/j.cemconcomp.2019.02.016.

[9] Li, Y., Zhang, Y., Yang, E. H., & Tan, K. H. (2019). Effects of geometry and fraction of polypropylene fibers on permeability of ultra-high performance concrete after heat exposure. Cement and Concrete Research, 116, 168–178. https://doi.org/10.1016/j.cemconres.2018.11.009.

[10] Li, Y., Yang, E. H., & Tan, K. H. (2020). Flexural behavior of ultra-high performance hybrid fiber reinforced concrete at the ambient and elevated temperature. Construction and Building Materials, 250, 118487. https://doi.org/10.1016/j.conbuildmat.2020.118487.

[11] Lin, J., Zhang, Y., Huang, S., Wang, Y., & Zhang, Z. (2024). Influence of synthetic fibers on the performance of ultra-high performance concrete (UHPC) at elevated temperatures. Journal of Building Engineering, 97, 110735. https://doi.org/10.1016/j.jobe.2024.110735.

[12] Qi, R., Guo, R., Pan, T., Lin, R., Fu, C., & Liu, X. (2026). Enhancing spalling resistance and mechanical properties of ultra-high performance concrete at elevated temperatures using hybrid polyoxymethylene and steel fibers. Construction and Building Materials, 526, 146443. https://doi.org/10.1016/j.conbuildmat.2026.146443.

[13] Lee, K. J. L., Kevinly, C., & Tan, K. H. (2026). Effect of hybrid fibre on flexural behaviour and spalling resistance of ultra-high performance fibre-reinforced concrete at ambient and elevated temperatures. Construction and Building Materials, 517, 145670. https://doi.org/10.1016/j.conbuildmat.2026.145670.

[14] GB/T 50080-2016. (2016). Standard for test method of performance on ordinary fresh concrete.

[15] GB/T 31387-2015. (2015). Reactive powder concrete.